

Structural repairing of damaged reinforced concrete beam-column assemblies with CFRPs

Özgür Yurdakul^{*1} and Özgür Avşar^{2a}

¹Jan Perner Transport Faculty, University of Pardubice, Pardubice, 53009, Czech Republic

²Department of Civil Engineering, Anadolu University, Eskişehir, 26555, Turkey

(Received October 28, 2014, Revised February 4, 2015, Accepted February 6, 2015)

Abstract. Depending on the damage type as well as the level of damage observed after the earthquake, certain measures should be taken for the damaged buildings. In this study, structural repairing of two different types of damaged RC beam-column assembly by carbon fiber-reinforced polymer sheets is investigated in detail as a member repairing technique. Two types of 1:1 scale test specimens, which represent the exterior RC beam-column connection taken from inflection points of the frame, are utilized. The first specimen is designed according to the current Turkish Earthquake Code, whereas the second one represents a deficient RC beam-column assembly. Both of the specimens were subjected to cyclic quasi-static loading in the laboratory and different levels of structural damage were observed. The first specimen displayed a ductile response with the damage concentrated in the beam. However, in the second specimen, the beam-column joint was severely damaged while the rest of the members did not attain their capacities. Depending on the damage type of the specimens, the damaged members were repaired by CFRP wrapping with different configurations. After testing the repaired specimens, it is found that former capacities of the damaged members were mostly recovered by the application of CFRPs on the damaged members.

Keywords: CFRP; beam-column joint; reinforced concrete; structural repair

1. Introduction

Each damaging earthquake in Turkey (Marmara 1999, Bingöl 2003, Van 2011) demonstrated the inadequate seismic performance of improperly designed and constructed reinforced concrete (RC) frames. Some of the main reasons for this appear to be the insufficient control mechanism, improper applications during design and construction stages and inadequate material properties. Low concrete strength (in some structures as low as 8-10 MPa), inadequate or no transverse shear reinforcement in the member ends and beam-column joints, longitudinal reinforcement bond problems due to use of plain round bars and improper hook detailing of bars are some of the most frequently observed deficiencies in the past earthquakes (Sezen *et al.* 2003, Doğangün 2004, Yılmaz and Avşar 2013, Avşar and Tunaboyu 2014). As a result, RC frames containing some of the indicated deficiencies, may be exposed to brittle type of failure at local level such as failure of

*Corresponding author, Graduate Student, E-mail: ozgur.yurdakul@student.upce.cz

^aAssociate Professor, E-mail: ozguravsar@anadolu.edu.tr



(a) L'Aquila-Italy (2009) Earthquake

(b) Simav-Turkey (2011) Earthquake

Fig. 1 Beam-column joint shear failure

beam-column joint. This can result in moderate to severe structural damage or even the total collapse of moment-resisting frame buildings (see Figs. 1(a)-(b)). RC buildings with moderate to severe structural damage after the earthquakes should be demolished or repaired depending on the damage level. Different techniques exist to repair the damaged RC buildings according to their damage level. Repairing the non-structural components can be sufficient for lightly damaged RC buildings. Moderately damaged RC buildings can only be serviceable after the application of sufficient structural repairing techniques.

Even though there are sufficient number of studies on well-detailed beam-column joint (Kotsovou and Mouzakisi 2012, Lee *et al.* 2009, Haach *et al.* 2008, Burak and Wight 2004, Canbolat and Wight 2008), there exists limited number of contributions on the joints which were constructed according to pre-1970s construction practice (Antonopoulos and Triantafillou 2003, Bindhu *et al.* 2008, Hassan 2011). Deficient RC buildings in Turkey were not fully represented by these studies although they did not comply with any code requirements. Nevertheless, studies considered some of the existing deficiencies of Turkish buildings resulting from lack of shear reinforcement in the joint and poor material properties including low strength concrete and the presence of plain round reinforcement bars were conducted by Bedirhanoglu *et al.* (2010), İlki *et al.* (2011), Coskun *et al.* (2012). According to the results of these studies, it is emphasized to take necessary precautions for such buildings with the previously indicated deficiencies. Therefore, researches focus on not only the behavior of RC beam-column joints under seismic loading, but also strengthening of insufficient members. For this reason, in early stage of strengthening of beam-column joint studies, researchers conducted several tests with the available construction materials such as steel jacketing by using structural steel, joint enlargement with concrete, using an additional reinforcement material in the joint (Alcocer and Jirsa 1991, Karayannis *et al.* 1998, Biddah *et al.* 1997, Mahini and Ronagh 2010, Fisher and Sezen 2011). Due to emerging technologies on construction materials in recent years, researchers tend to study on new retrofit materials like fiber-reinforced polymers (FRP) (Le-Trung *et al.* 2010, Lee *et al.* 2010, Parvin and Granata 2000, Ghobarah and El-Amoury 2005, Ghobarah and Said 2002, Parvin *et al.* 2010, Del Vecchio *et al.* 2014, Hadi and Tran 2014, Topçu 2008, Akgüzel and Pampanin 2010, Coşkun *et al.* 2012). Also, in the previous studies, the effectiveness of the application of fiber-reinforced polymer (FRP) sheets as a seismic repairing technique was investigated through repairing of a

certain locally damaged RC beam-column joint for a certain damage level (El-Amoury and Ghobarah 2002, Ghobarah and Said 2001, Garcia *et al.* 2014, Engindeniz 2008, Elsouri and Harajli 2015, Li and Kai 2011, Karayannis *et al.* 2008, Karayannis and Sirkelis 2008). However, in the present study, the efficiency in repairing the damaged RC beam-column assembly components with CFRPs was investigated by considering the two different damage types. Two different beam-column assemblies with the same geometry but different material properties and detailing were investigated to consider different damage types with varying damage level. Depending on the damage type, the assemblies were repaired by CFRPs with different configurations accordingly.

The objective of this study is to investigate the behavior of beam-column assembly and the effectiveness of different repairing techniques to moderately and severely damaged RC components by CFRP sheets. For this purpose, two types of exterior RC beam-column assembly test specimens were utilized. The first test specimen was designed according to the current earthquake code in Turkey and the second one represents the beam-column assembly of a deficient RC building which has certain deficiencies at joint level such as improper material quality and lack of transverse reinforcement in the beam-column joint. Therefore, response of two different test specimens and different repairing techniques, which were applied to the damaged RC components exposed to different damage type, were compared and their effectiveness was investigated in detail.

2. Experimental program

2.1 Test specimen details and materials

Two full scale test specimens, which represent the exterior beam-column assembly taken from the inflection points of the frame, were tested (see Fig. 2). The top end of the column was subjected to quasi-static reversed cyclic loading, which is considered to be the representative

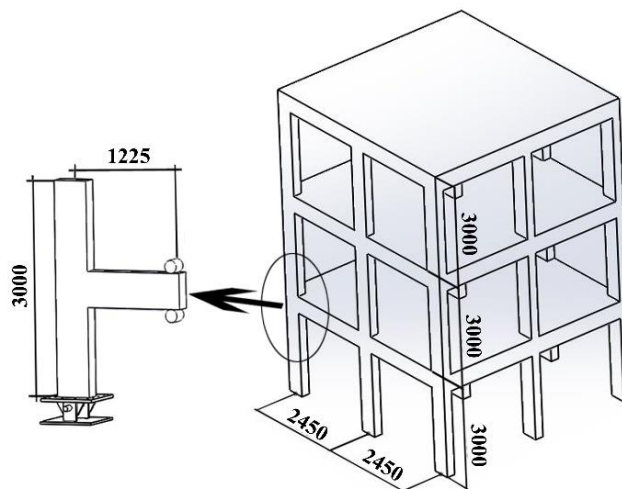


Fig. 2 Test specimens in model building

earthquake force. The column ends of the assembly were detailed such that they become zero-moment joints like a pin support. The right end of the beam was supported by roller supports so that beam end joint can freely move in the horizontal direction.

The first beam-column assembly test specimen (E001) was designed according to current Turkish Earthquake Code (TEC 2007). The first test specimen had column dimensions of 250×500×3000 mm, the column was connected to half-length beam with dimensions of 250×500×1500 mm at mid-span (see Fig. 3(a)). The longitudinal reinforcement ratio of column and beam were 1.22% and 1.61% respectively. 16 mm and 18 mm diameter deformed bars were used in the column and beam. 8 mm diameter deformed bar with 135-degree hooks was used as transverse reinforcement in the beam and column. They are placed with a spacing of 75 mm and 50 mm at the confinement regions of column and beam, respectively. But for the unconfined regions, the transverse reinforcement spacing was selected as 150 mm and 95 mm for the column and beam, respectively. Since the first specimen was designed according to the earthquake code in action, transverse reinforcements are placed in the beam-column joint. According to TEC (2007), minimum concrete compressive strength is 20 MPa and it was selected as a target compressive strength for the first test specimen, E001.

The second test specimen (E002) represents the deficient beam-column assembly, which is very common in most of the existing buildings that were constructed before 1999 in Turkey. The second specimen was non-conforming to the current and former earthquake design code principles. The same geometric dimensions with the first specimen were also selected for E002. The longitudinal reinforcement ratio of column and beam were 1.63% and 2.04 % respectively. 18 mm diameter plain round bars were used in the column and beam. 10 mm diameter undeformed bar with 90-degree hooks were used as a transverse reinforcement (see Fig. 3(b)). In the second specimen, there was no transverse reinforcement in the beam-column joint region and the concrete compressive strength was expected around 8-10 MPa. The maximum aggregate dimensions are selected to be between 5 mm to 12 mm for the concrete mixture design of low concrete strength. In order to investigate the seismic behavior of RC beam-column assembly for the reference and repaired test specimens, the minimum required axial load for columns according to TEC (2007), which is $0.1A_c f_c^*$, was used for both specimens. Because the axial load increase the joint shear strength, the axial load applied to the columns was selected to be the minimum to consider the most critical case. Mechanical properties of materials and applied axial load for each reference specimens (E001 and E002) as well as the repaired test specimens (E001-R and E002-R) were summarized in Table 1.

In the previous studies, the failure mechanisms of such specimens mostly include two failure modes which are shear failure in the joint and slippage of beam longitudinal reinforcement bars

Table 1 Properties of the test specimens

Test Series	Specimen Number	Mechanical Properties			Joint Transverse Reinforcement	Axial Load $N=0.1A_c f_c^*$ (kN)
		Concrete Compressive Strength, f_c^* (MPa)	Steel Yield Stress, f_y (MPa)	Steel Ultimate Stress, f_u (MPa)		
Series 1	E001	19.14	522.00	784.00	Present	240
	E001-R					
Series 2	E002	8.05	292.50	437.50	N/A	100
	E002-R					

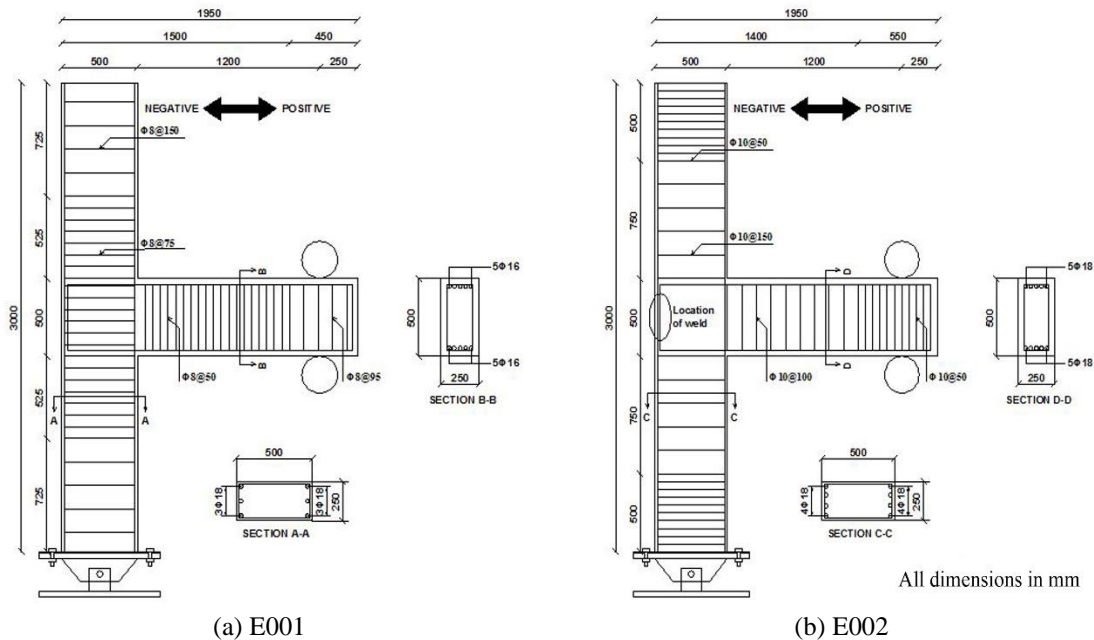


Fig. 3 Dimensions and reinforcement detailing

and then slippage failure dominates the other types of failure modes when plain bars were used (İlki *et al.* 2011). However, bond slip failure can be partially prevented even in the existing buildings by removing the concrete cover in the back of column, welding the column longitudinal reinforcement bars to the hooks of beam reinforcement bars and repairing with mortar (İlki *et al.* 2011). The slippage failure modes therefore can be switched to the other failure modes. In this study, the hooks of longitudinal beam bars were welded to column longitudinal bars in the second specimen to prevent failure due to slippage (see Fig. 3(b)). There are two reasons to exclude the slippage problem in E002. Due to the presence of deformed bars in the first specimen (E001), the slippage problem is very limited. In order to be consistent in comparing the results of both specimens, a failure mechanism due to slippage in the second specimen was prevented (E002). The second reason is that it is not practical to eliminate slippage problem by externally applied CFRPs only. In order to investigate the effectiveness of repairing by CFRPs, occurrence of slippage problem is intended to be minimized through welding of beam and column reinforcement bars.

After testing the reference specimens up to 4% drift ratio under cyclic loading, they were structurally repaired by CFRPs after certain level of damage which corresponds to moderate damage for E001 and severe damage for E002 penetrated in the critical components of beam-column assemblies. The CFRP sheet that was used in repair had an elasticity modulus of 230,000 MPa, 0.111 mm thickness, 2.10% ultimate strain and 4900 MPa ultimate tensile strength. Before applying CFRPs, repair mortar with 28-day compressive strength of 60 MPa was used to fill the cracks, which were formed in the critical components due to the initial testing of beam-column assemblies.

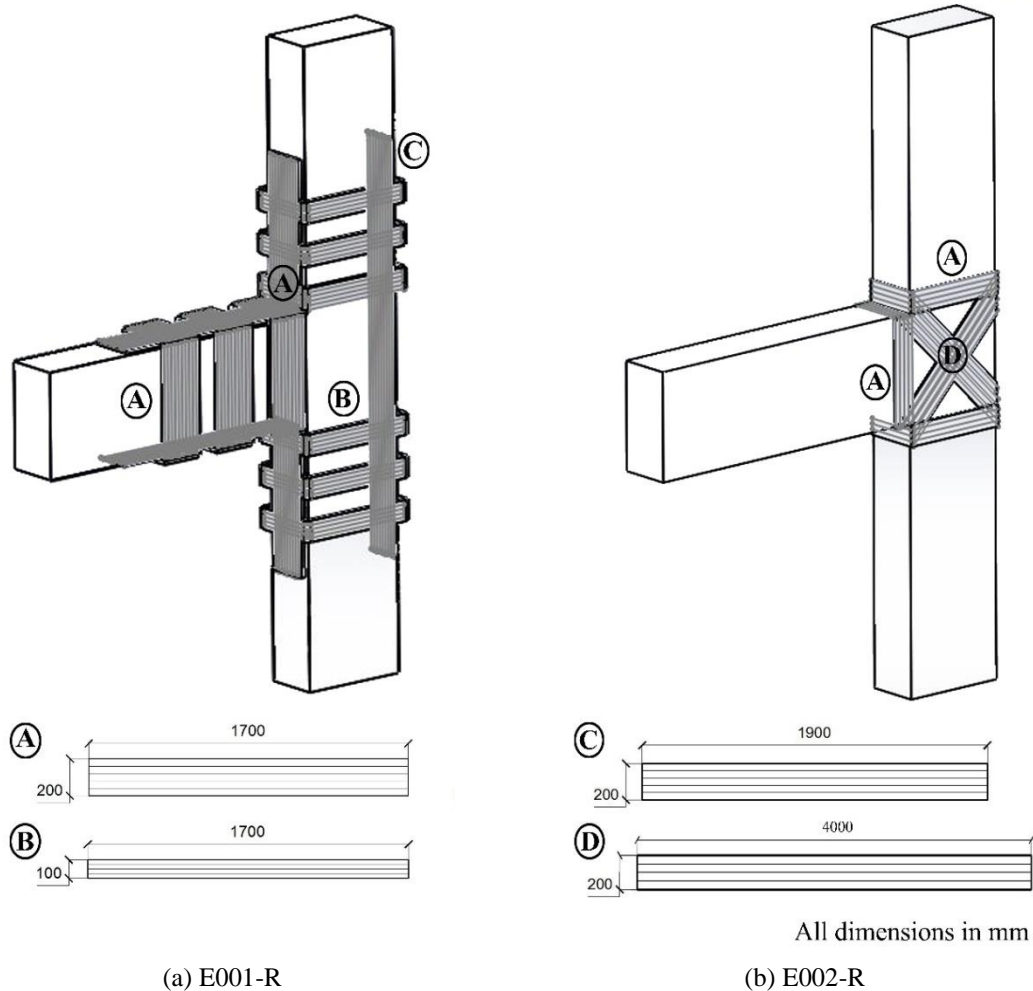
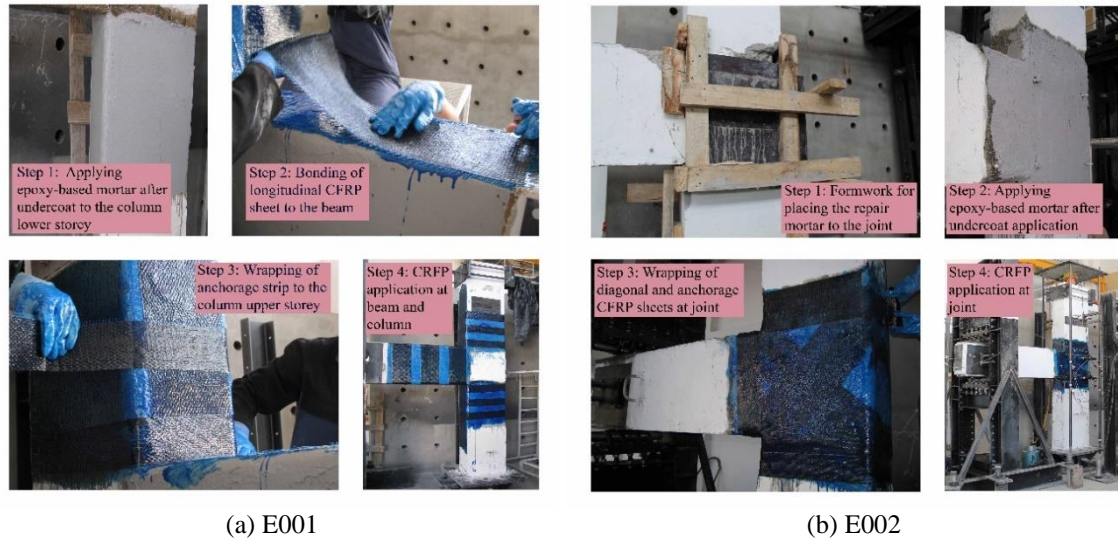


Fig. 4 Schematic representations of CRFP repairing

2.2 Structural repair design

The design philosophy of repair for initially damaged specimens is to attain the initial capacity, upgrading the seismic performance of damaged components, delaying or eliminating brittle failure modes and initiating the formation of flexural plastic hinges in the beam to attain a ductile behavior (El-Amoury and Ghobarah 2002). After testing the reference specimens, the deficiency of members were realized and two different types of repairing techniques considered. In the first specimen (E001) beam and column members and in the second specimen (E002) beam-column joint were repaired by CFRP wrapping. In designing the dimensions of CFRP sheets, it is assumed that the entire lateral load exerted on the damaged test specimen will be carried by the corresponding CFRP sheets.

A ductile performance was observed in E001 specimen and plastic hinges took place in the beam. For this reason, a one layer CFRP with 200 mm width was applied to the top and bottom



(a) E001 (b) E002
Fig. 5 Repairing process of specimens as shown in Figs. 4(a)-(b)

surfaces of beam and anchored by three CFRP sheets with 200 mm width, 1700 mm length (see Fig. 4(a)). The sheets used for anchoring were placed at 100 mm in transverse direction. These transverse direction CFRP sheets also increased the shear resistance of the beam. For a ductile behavior of the specimen, plastic hinges are expected to occur in the beam. Since the beam was repaired, strong beam weak column case could occur. Then, the flexural capacity of column could be exceeded before the beam reached to its flexural capacity. For this reason, while the beam was repaired, the column was repaired as well. A one layer CFRP with 200 mm width was applied at the front and back surfaces of upper and lower story columns. Six 100x1700mm CFRP sheets were placed in the transverse direction with spacing of 100 mm to anchor longitudinal CFRPs and to increase the shear capacity of the column. It was known from the experiment of E001 that, the member capacities could not exceed the beam-column joint capacity for this specimen. Therefore, no repairing action was taken for the beam-column joint.

The failure mechanism was brittle joint shear failure for E002 specimen. Therefore, joint region was repaired to attain the initial shear capacity of the joint. Before the application of CFRPs, spalled concrete at the joint was removed after testing E002. Then, repair mortar was placed in place of removed concrete in the joint. Two layers of CFRP sheets with 200 mm width and 4500 mm length were orientated $\pm 45^\circ$ with respect to beam axis. These diagonal sheets were anchored to the beam and column at upper and lower story level by means of three 200x1700 mm CFRP sheets by wrapping the RC components with a single layer of CFRP (see Fig. 4(b)).

Wrapping the CFRPs in the form of X pattern can be implemented in case of exterior joints with floor slab and transverse beams (Coskun *et al.* 2012). Therefore, proposed CFRP wrapping technique can be considered as a viable solution for on-site construction operations. CFRPs were used for E001 and E002 specimens as a repairing material as discussed before. Application of CFRPs started with rounding the section corners to prevent the tearing of CFRP sheets due to sharp corners of the RC sections. Then, a thin layer of undercoat was applied on the corresponding RC component to be repaired. After that, epoxy based repair and anchorage mortar was applied to obtain smooth surface. Finally, CFRP sheets were saturated with epoxy and applied to the

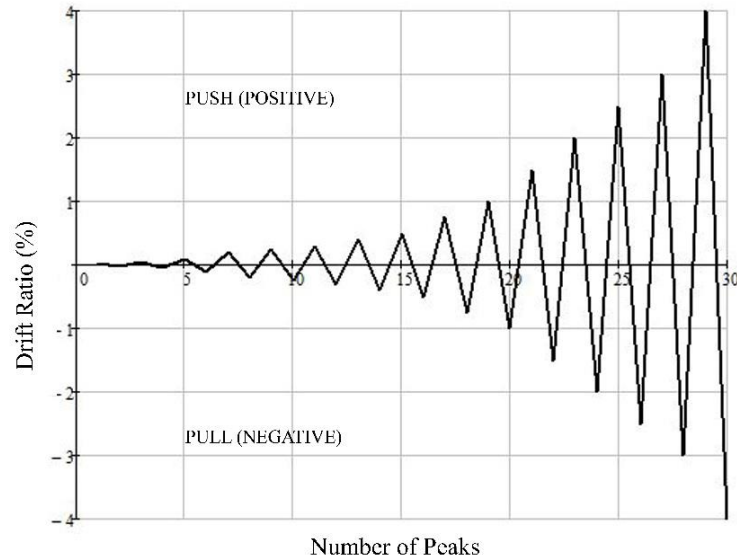


Fig. 6 Test sequence of displacement controlled cycles

corresponding member surface. In order to get a good bonding between CFRP sheets and surfaces, a hand roller was used to remove air and stick them properly (see Figs. 5(a)-(b)).

While making the structural repair design of the damaged members of the first test assembly (E001), it is assumed that the force acting on the beam longitudinal reinforcement bars due to flexural moment was resisted by only CFRP sheet. In the second test assembly (E002), the amount of diagonal CFRP sheet was determined such that the tension force in the beam-column joint should be less than the tension force capacity of the diagonal CFRP sheet.

2.3 Instrumentation, test setup and loading procedure

A series of laboratory tests were performed at Structural Mechanics Laboratory, Department of Civil Engineering, Anadolu University. In these tests, quasi-static cyclic lateral displacement was applied from top of column under the combined action of constant column axial load so that the real behavior of beam-column assembly can be investigated in the laboratory. Lateral displacements were carried out until reaching the expected drift ratios (see Fig. 6). Notified drift ratios are the ratio of measured lateral displacement to the distance between the point of application of lateral displacement and bottom of lower story column.

The column was positioned vertically and supported by pin support at bottom end. In order to connect the pin support to column, six 40×40×4 mm equal length angles with 400 mm length were welded to firstly 800×800×10 mm plate, which is called as column bottom plate, then to column longitudinal bars and hooks. After that, the column bottom plate was connected with eight 30 mm bolts to the top plate of pin support. The beam was positioned horizontally and supported by roller support at the end. The roller support was provided by seven cylindrical rolling bearing units. Once each bearing units were subjected to concentrated loads, there was a risk of concrete crushing due to bearing stress developed at the beam end. To overcome this undesirable situation, two 250×500×30 mm plates were welded to beam top and bottom longitudinal bars. Axial and

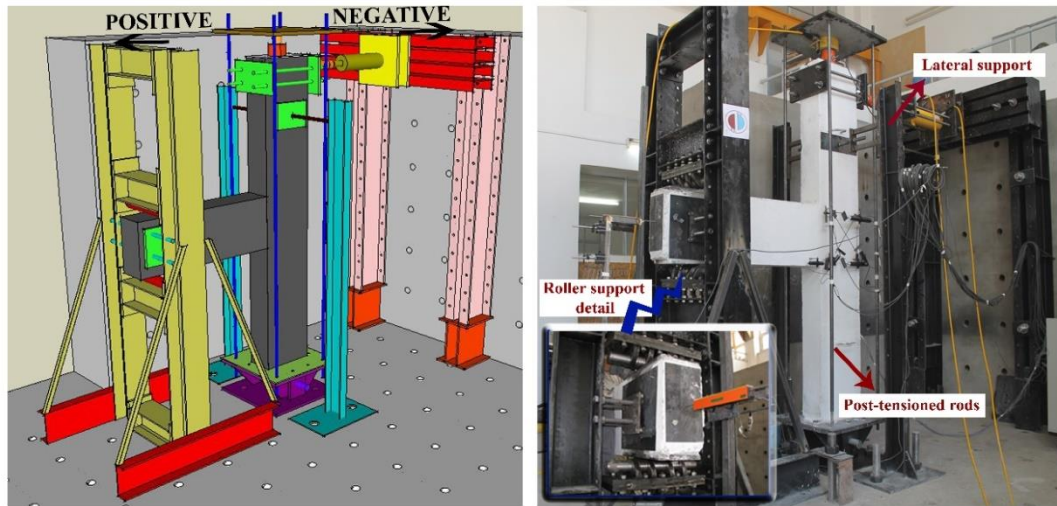


Fig. 7 3D view of test setup

lateral loads were applied by a single-acting and double-acting hydraulic cylinder respectively. Double-acting hydraulic cylinder was placed to an adjustable steel frame that allows movement in both horizontal and vertical direction and the steel frame was fixed to reaction wall. The single-acting hydraulic cylinder was fixed to 800x800x30 mm plate at the top of the column. This plate was connected to top plate of pin support by four 3500 mm longitudinal rods. Axial load was applied by means of four vertical post-tension rods placed between the pin support and plate over the top of the column supporting the hydraulic cylinder acting vertically. Since axial load was always in the direction of column axis, constant axial load in push and pull cases was observed in the early stage of lateral displacement. Due to the formation of cracks and crushing of concrete, axial load was controlled to keep it constant in the subsequent drift levels. The specimens were laterally supported by bearing units from end of beam and top of column to prevent out of plane movement (see Fig. 7).

Thirteen strain gage-based linear variable differential transducers (LVDTs) were used to measure the lateral displacements at top of column and story level, the shear deformations of joint, horizontal movement and rotation of pin support, slippage of beam (see Fig. 8(a)). The strain levels of reinforcement bars were measured by fifteen unidirectional strain gauges (see Fig. 8(b)). Also, one tension compression and one compression load cell were used to measure the lateral load and the axial load applied at the top of the column, respectively (see Fig. 8(a)).

3. Experimental results and discussion

The horizontal responses of both specimens were examined and the overall performance of reference specimens was compared with the corresponding repaired specimens. The damaged photographs of specimens at 4% drift ratio are illustrated in Figs. 9(a)-(b). The column lateral tip load versus drift ratio and envelopes of hysteretic loops for all specimens are plotted in Figs. 10-11, respectively. Also, the significant steps in the experiments such as cracking, debonding and fracture of CFRPs, concrete spalling are also indicated in the graphs shown Fig. 10. Observed

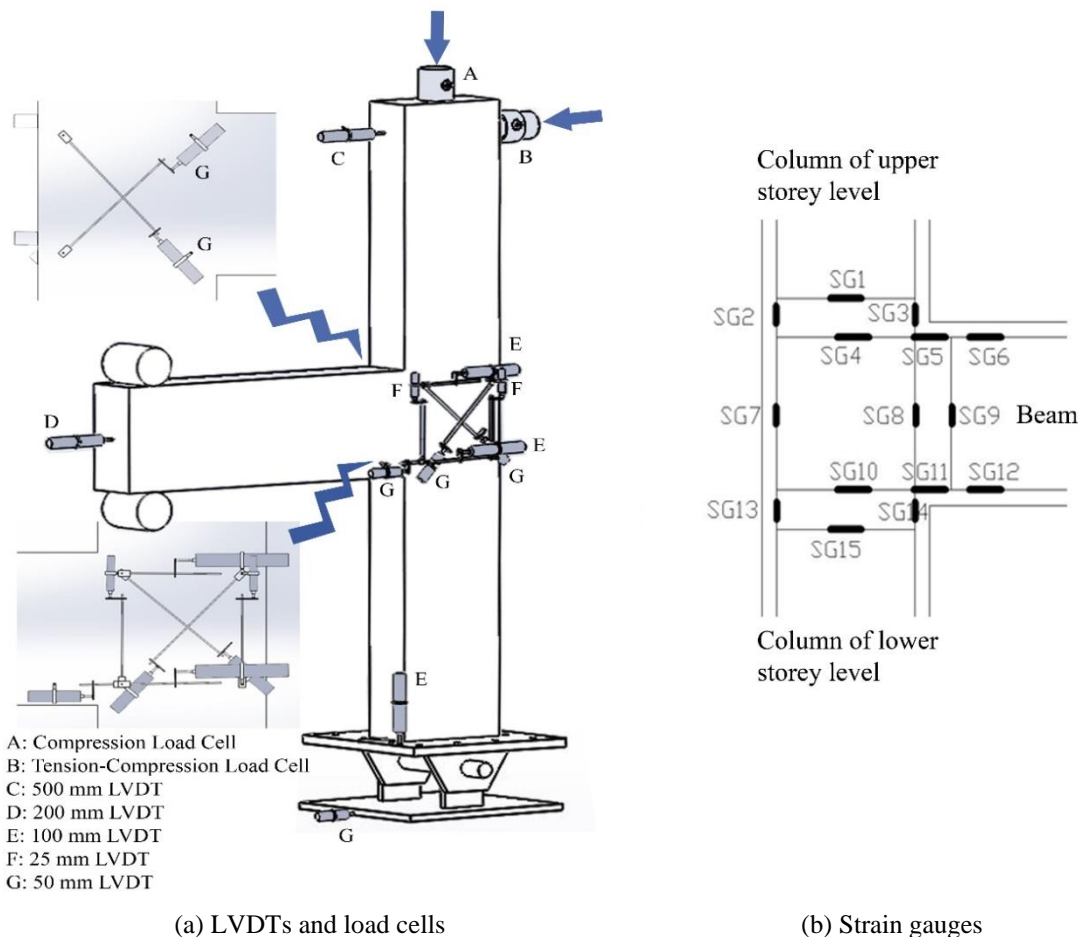


Fig. 8 Location of measuring instruments in 2D and 3D view

results for the effectiveness of repairing by different CFRP configuration are compared and discussed through the response quantities such as strength, stiffness, stiffness degradation and energy dissipation capacity of the specimens. The test results are summarized in Table 2. E001-R and E002-R correspond the repaired specimens E001 and E002, respectively.

3.1 Hysteretic response of the specimens

In the first specimen (E001), a ductile response was observed through the strain gauge measurements as the longitudinal reinforcement bars of the beam yielded before any type of failure, which is an expected behavior for E001. The computed plastic flexural capacity of beam, which corresponds to the lateral force capacity of the beam-column assembly, is 110 kN and the beam member reached that value with the global yielding of the assembly (see Fig. 10(a)). The first flexural crack at beam was observed at 0.25% drift ratio which corresponds to 17.5% of maximum load before yielding the beam longitudinal bars. Due to the presence of deformed bars in accordance with the code requirements, the flexural and shear cracks were extended to almost

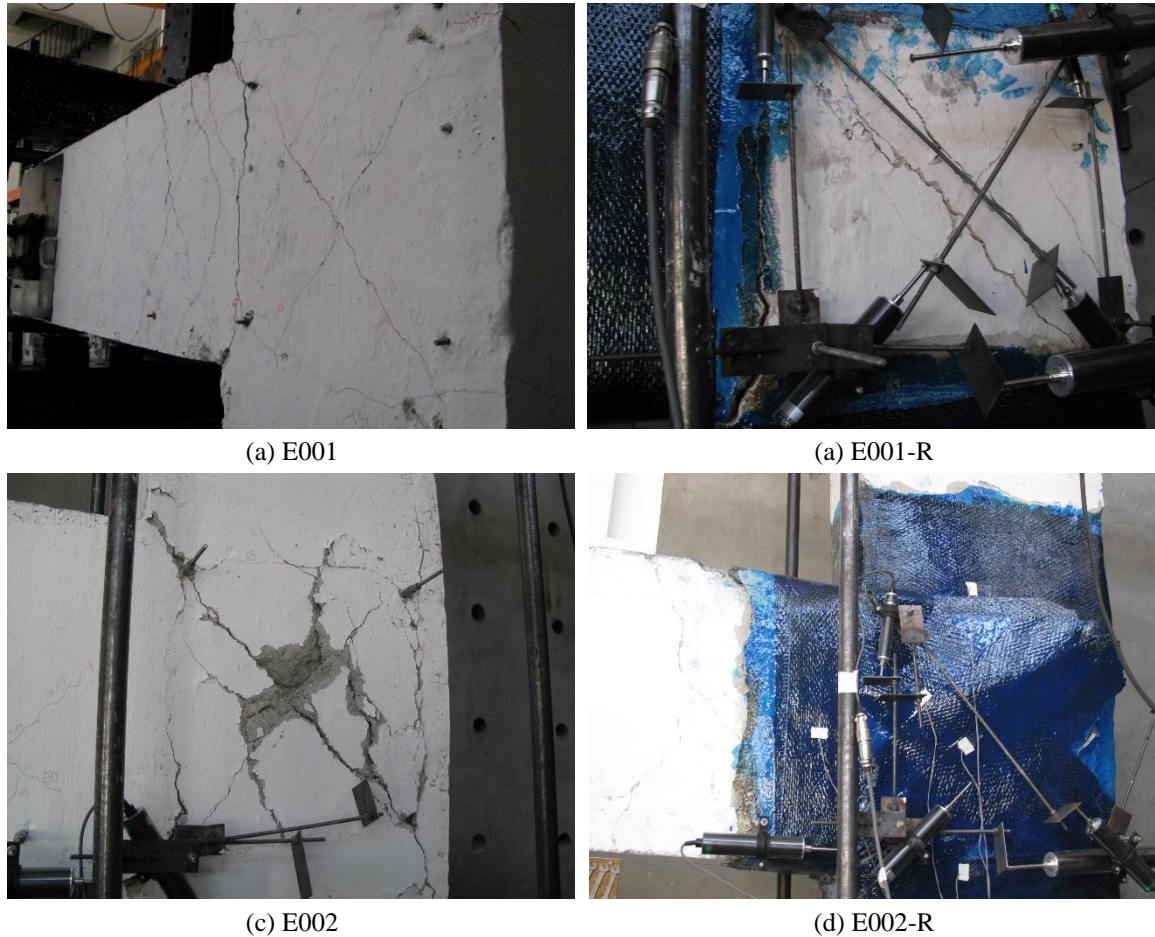


Fig. 9 Damaged photograph of specimens at 4% drift ratio

whole beam length evenly and plastic hinge initiated at beam joint interface due to flexure. The first observed inclined joint crack was at 0.50% drift ratio. Then, although the flexural capacity of beam did not exceed the joint shear capacity, hairline cracks in the joint were observed but these cracks in the joint did not widen. In the last loading stages of the specimen, hairline flexural cracks developed in the column but it did not affect the behavior of the specimen.

For specimen E001-R, the failure mode under cyclic loading was almost similar with E001. During the first few cycles, hairline cracks at the joint and flexural cracks at the beam joint interface that occurred during experiment of specimen E001 were widened. However, the other cracks in the column and beam from E001 test could not be observed due to cover of CFRP sheets. The first CFRP debonding initiated at 0.50% drift ratio which corresponds to 29.5% of maximum load at beam joint interface. After a few cycle later, the first CFRP fracture started around the debonding region at 1.00% drift ratio. By increasing the column lateral tip displacement, the CFRP was ruptured, the existing flexural crack at interface and shear cracks at joint enlarged and spalling of concrete cover also took place at the beam-column interface as observed at E001 in a similar way.

Unlike the first test series, the behavior of specimens E002 and E002-R was a brittle shear failure of the joint. The capacity of the specimens was limited by joint strength. The first flexural crack at beam, beam-joint interface and first inclined crack at the beam-column joint was observed at the same drift ratio, 0.20%, which formed at 29.5% of the ultimate load in the test of E002. As the imposed displacement increased, new cracks occurred at 0.5% and 1.5% drift ratios at joint parallel to the beam and column respectively. With the increase in the drift ratio of the beam-column assembly, widening of shear cracks at joint increased, and the concrete in the joint core crushed and spalled. Even though, the hooks of beam longitudinal bars were welded to column longitudinal bars, slippage problem was not fully prevented. As a result of slippage at the beam, welded hooks of beam longitudinal bars cause buckling of the column longitudinal bars and they did not keep their right angle anymore. The concrete cover at back side of column in the joint also spalled due to deformation of beam longitudinal reinforcement hooks at the beam end. Also, the shear and flexural cracks did not spread to the whole length of the beam (see Fig. 9(c)). The cracks were generally concentrated at the beam-column joint and beam-column interface. A large flexural crack initiated at the beam-column interface and the crack width widened with the increasing drift ratio due to presence of plain round bars in the beam. The plastic flexural capacity of the beam for E002 specimen, which corresponds to the lateral force capacity of the beam-column assembly, is 69 kN determined from section analysis. As shown in Fig. 10(c), the hysteretic response of E002 obtained from the test did not reach to beam flexural capacity. For this reason, the ductile behavior could not be observed due to the fact that the beam-column joint reaches to its shear capacity before the beam attains its flexural capacity.

The observed failure mode of E002-R was shear failure at joint as also observed for the reference specimen, E002. The performance of repaired specimen was quite satisfactory until debonding of the diagonal CFRP sheets on the joint surface. The first CFRP debonding was observed at 0.40% drift ratio which corresponds to 50% of maximum lateral load. However, the flexural crack was observed in the beam at 0.20% drift ratio which is before the occurrence of CFRP debonding. This implies that the application of diagonal CFRPs at the beam-column joint has changed the behavior of the beam-column assembly and flexural deformations in the beam dominated the overall response before the fracture of CFRPs. After several cycles of the first debonding, fracture of the CFRPs was initiated as shown in Fig. 9(d).

The reason of failure in the E002-R specimen was the fracture of diagonal CFRPs (see Fig. 9(d)) and as a consequence the spalling of repair mortar at joint core was occurred. The first CFRP fracture at joint occurred at 2% drift ratio. After this point, the capacity of the repaired specimen was diminished by the shear failure of the beam column joint leading to a brittle type of failure. In the design of CFRP sheets for repairing the damaged E002 specimen, two layers of CFRP sheets with 200 mm width was selected to be applied diagonally at the beam-column joint. In the design stage, the full CFRP sheet area was considered to be in tension. However, one side of the CFRP sheet was exposed to larger stress due to the eccentricity and hence total CFRP section did not work as it was designed. This led to tearing of the CFRP sheet from one side that had higher axial stress. Therefore, it is inferred that more layers of diagonal CFRP sheets should have been used for the applied repairing technique to be more effective for the higher drift ratios. Even the application of two layers of CFRP sheets with 200 mm width result in more flexural deformations in the beam leading to a more ductile behavior compared to the reference specimen. Propagation of flexural cracks was in the uncracked beam sections as well as widening of crack width in the existing cracks observed in the repaired specimen before the fracture of diagonal CFRPs.

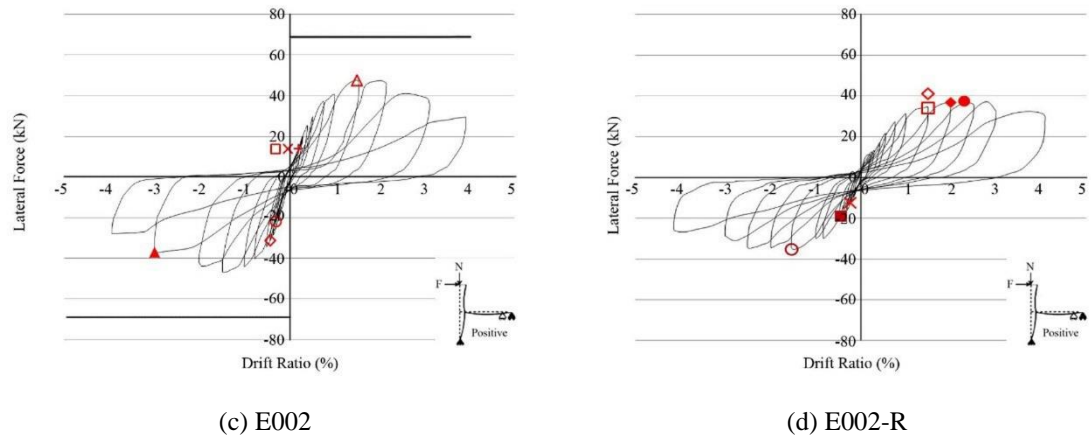
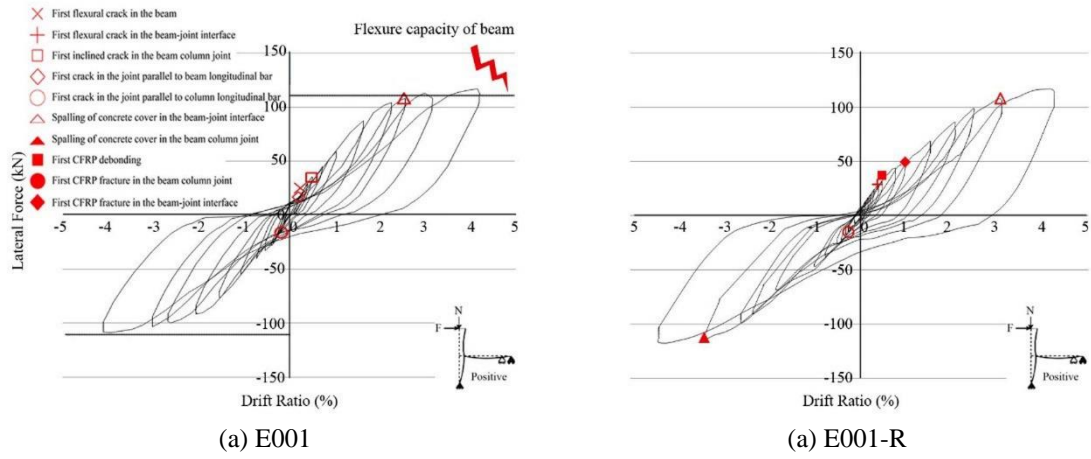


Fig. 10 Maximum lateral load vs. drift ratio graphs for specimen

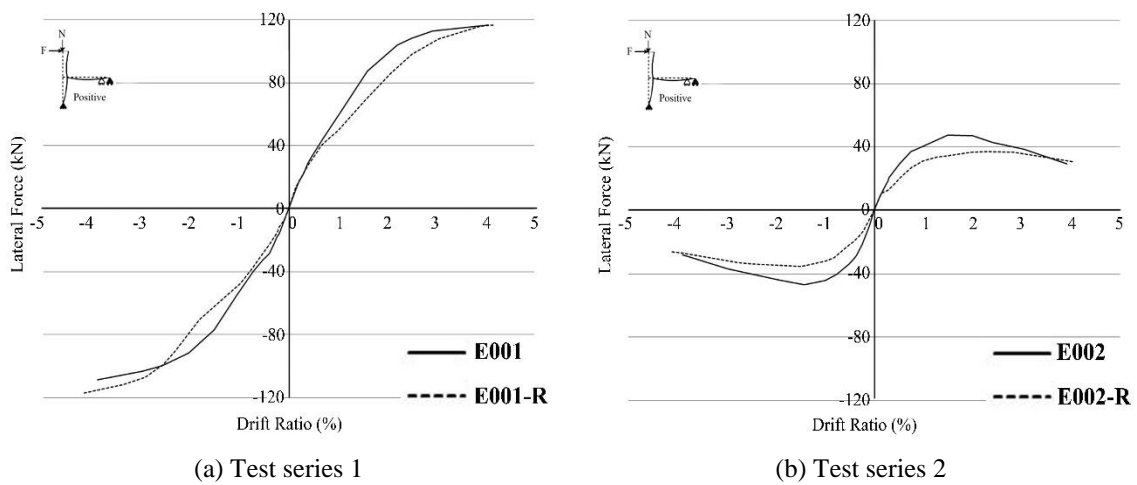


Fig. 11 Envelope curves of hysteretic loops

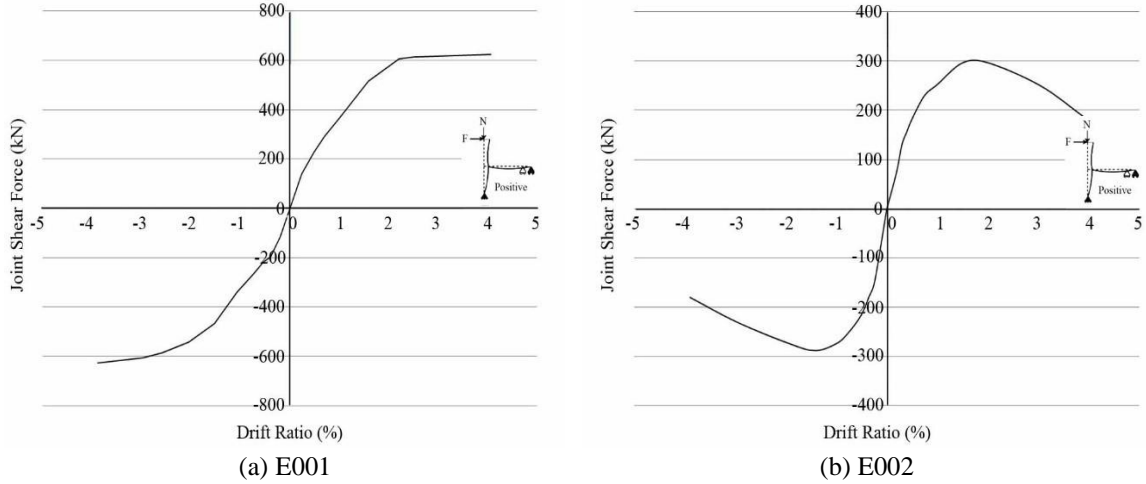


Fig. 12 Joint shear force vs. drift ratio responses

3.2 Strength and joint shear strain

Strength and joint shear strain are the important parameters that indicate the effectiveness of the repairing technique applied for the specimens. The strength parameters were discussed in terms of maximum horizontal load applied at the assembly and the joint shear force that obtained from experimental results. The applied maximum horizontal forces are quite similar with reference (E001) and repaired (E001-R) specimens of test series one. As shown in Fig. 11(a), the backbone curve of the repaired specimen is very close to the reference specimen, which verifies the effectiveness of the applied repairing scheme for the damaged specimen (E001). However, once the results were compared for the second reference specimen (E002), the repaired specimen of the second test series had a 22% and 25% lower value in positive and negative directions, respectively (see Fig. 11(b)). As discussed before, the maximum horizontal load capacity of the repaired specimen (E002-R) did not attain the corresponding capacity for the reference specimen due to the fracture of diagonal CFRP sheets. One can conclude that the repairing technique applied for the damaged E002 sample is not effective enough in terms of the horizontal load capacity of the beam-column assembly. However, it should be noted that depending on the number of diagonal CFRP sheet layers, the fracture of the CFRP sheets is expected to take place in higher drift ratios with the attainment of greater horizontal load capacities.

The second significant strength parameter is the joint shear force that was calculated from experimental results by using Eq. (1).

$$V_j = V_b - V_c \quad (1)$$

V_j , V_b , V_c denotes the joint shear force obtained from experimental results, the forces in the longitudinal reinforcement of beam obtained from measured data in strain gauges that located in the beam longitudinal bars and the horizontal load applied at the beam-column assembly, respectively. The joint shear forces are determined only for the reference specimens (E001 and E002) in both test series. Because after testing the reference specimens up 4% drift ratio, the strain

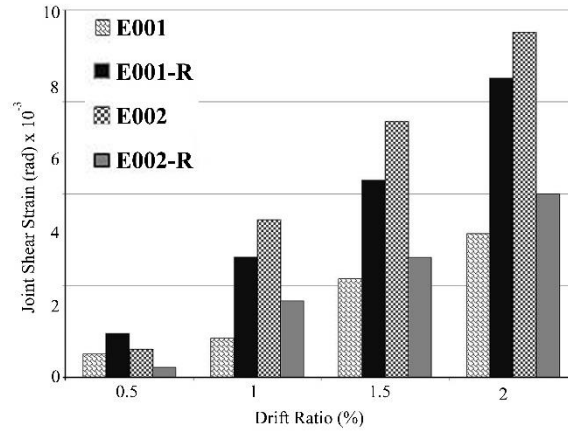


Fig. 13 Joint shear strain vs. drift ratio

gauges are not functional anymore due to rupture or separation from the reinforcement surfaces to which they were attached. Therefore, no data could be collected from strain gauges after testing the reference specimens. The joint shear force versus drift ratio is plotted in Figs. 12(a)-(b). These curves are in good agreement with the corresponding backbone curves presented in Figs. 11(a)-(b). The joint shear capacity of the first specimen, which was designed in accordance with TEC (2007), is twice more than the second specimen without exhibiting any deterioration.

Experimental joint shear stress was obtained by dividing the shear force to the joint area as given in Eq. (2). However, the failure mechanism of joint was due to diagonal cracks. Therefore, principal normal stresses at joint should be calculated by using Mohr Theorem to obtain maximum and minimum stresses which are normal and parallel to the diagonal cracks and represent the compression (σ_c) and tensile (σ_t) joint stresses. The joint stresses obtained from the experimental results in terms of shear, tensile and compression stresses were summarized in Table 2. The results indicate that the stresses determined for the first specimen (E001) is more than twice the stresses calculated for the second specimen. However, the diagonal cracks were limited in the beam-column joint of E001 due to the presence of joint transverse reinforcements. On the other hand, the joint tensile stresses were resisted only by the tensile strength of concrete at the beam-column joint of E002. Once the concrete tensile strength was exceeded, diagonal shear cracks occur in the joint. Since there was no joint transverse reinforcement in E002, brittle type of joint shear failure was inevitable. This observation clearly indicates the importance of joint transverse reinforcement for a ductile behavior.

$$\tau_j = \frac{V_j}{A_c} \tag{2}$$

Joint shear strain is computed by using cosine theorem with the Eq. (3) in terms of radian. The displacement measurements obtained from horizontal, vertical and diagonal LVDTs at the beam-column joint were substituted in cosine theorem (Canbolat and Wight 2008).

$$\gamma = -\frac{\pi}{2} + \arccos\left(\frac{L_v^2 + L_h^2 - L_d^2}{2L_vL_h}\right) \tag{3}$$

Where L_v , L_h , L_d are obtained by summing the original length and measured displacement of vertical, horizontal and diagonal LVDTs respectively. The joint shear strain versus positive drift ratio graph was plotted in Fig. 13. The obtained result shows the effect of repairing on the joint response. The joint shear strains of E001-R are larger than its reference sample (E001). In the repaired specimen (E001-R), the beam and column capacities are improved with the addition of CFRPs while nothing was changed with the joint. In the reference specimen damage was concentrated in the beam. After repairing, damage was transferred to the beam-column joint, which resulted in an increase in the joint shear strains. For the second specimen, repairing by CFRPs at the deficient beam-column joint led to less joint shear strain for E002-R compared to reference sample, E002. This proves the effectiveness of diagonal CFRPs as a repairing technique for the damaged beam-column joints up to the fracture of CFRP sheets, which correspond to 2% drift ratio in this study.

3.3 Stiffness degradation and energy dissipation

The initial stiffness, K , of the specimens is defined as the slope of the line that joins the origin of backbone curve of the hysteretic response and the point where 60% of the ultimate lateral strength on the ascending part of the envelope curve. By using this approach, the initial stiffness values of specimens were calculated for both positive and negative direction as given in Table 2. The initial stiffness provided by CFRP in repaired specimens was lower than reference specimens due to imposed damage in the reference specimens. The ductility of the beam-column assemblies can be computed by dividing the ultimate horizontal displacement, Δ_u , to the yield displacement Δ_y . Since the ultimate displacement capacity of the first test specimen was not attained with the available test set-up for 4% drift ratio, ultimate displacement capacity of the first specimen could not be specified. Therefore, no comparison was made through the ductility capacity of the specimens. However, the equivalent yield displacement of each specimen was determined as given in Table 2 in terms of global drift ratio. To determine the yield displacement, an equivalent elasto-plastic force-displacement relation was obtained to represent the nonlinear backbone curve such that the area under both curves in other words energy absorption capacities are the same (Park 1989). As presented in Table 2, the equivalent yield displacement as well as the yield shear capacity of the first specimen is larger than the ones for the second specimen.

The peak to peak stiffness, K^p , is defined as the slope of line that connects the ultimate load points in positive and negative direction of hysteresis loop in each loading cycle. The normalized peak to peak stiffness with respect to reference specimens versus drift ratio curves is presented in Figs. 14(a)-(b). The peak to peak stiffness at each loading level decreased when the applied load devolved into inelastic range along with the increased level of damage. The sustained stiffness in each loading cycle of the reference specimens was higher than the repaired specimens due to existence of pre-formed cracks in the reference specimens. However, for drift ratios greater than 3%, the reference specimens could sustain the same level of peak to peak stiffness with the repaired specimens due to reduction in the contribution of CFRPs as a result of fracture.

The energy dissipation capacity during each loading cycle is computed to be the area enclosed within load-displacement curves. Then, the cumulative energy dissipated by specimens is obtained by summing the areas calculated for each loading cycle. The resulting cumulative energy versus drift ratio is shown in Figs. 15(a)-(b). The difference between the energy dissipation of E001 and E001-R is not more than 10% for each cycle. Therefore, repairing technique applied for E001 is considered to be effective in terms of energy dissipation. For the second specimen, energy

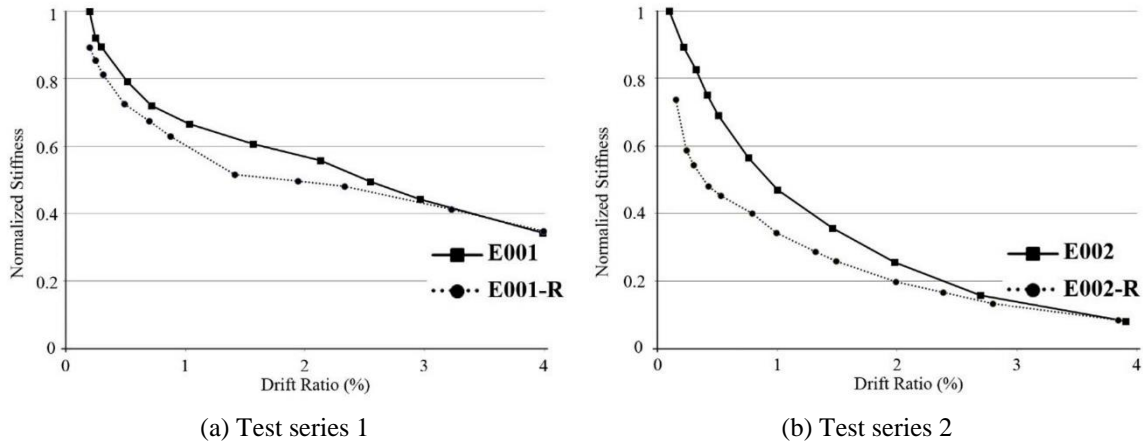


Fig. 14 Stiffness degradation curves

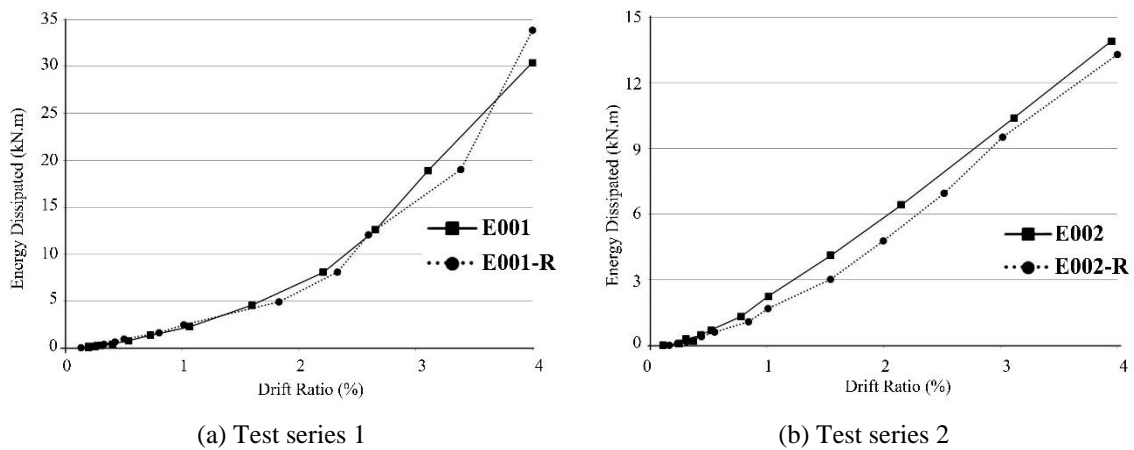


Fig. 15 Cumulative dissipated energy curves

dissipation capacity of the repaired specimen is always less than the reference specimen. As mentioned before, fracture of diagonal CFRP sheets result in less lateral force capacity and hence less energy dissipation capacity. If the fracture of CFRPs had been prevented by employing more layers of CFRPs, energy dissipation capacity of the repaired specimen expected to be higher than the reference specimen. At lower drift ratios, the energy dissipation capacity of E002 is larger than the repaired counterpart (E002-R) before the fracture of the CFRPs. This can be explained by the imposed structural damage in the repaired assembly occurred during the tests of the reference assembly.

4. Theoretical consideration and numerical solution

Theoretical shear capacity of joint is calculated by using truss analogy. Due to lack of shear reinforcement in the beam-column joint of E002, the failure of joint occurred by the formation of

Table 2 Summary of experimental results

Specimen	DOL *	Strength V_{max} (kN)	Yield Properties		Initial Stiffness K (kN/mm)	Energy E (kN.m)	Experimental Joint Stress (MPa)		
			V_y (kN)	Δ_y^* (%)			τ_j	σ_c	σ_t
E001	Pos.	117.00	111.97	1.97	1.97	30.40	5.19	6.24	4.32
	Neg.	108.75	97.70	1.73	1.77		5.02	6.08	4.16
E001-R	Pos.	116.85	112.95	2.60	1.54	33.87	N/A		
	Neg.	117.30	108.40	2.56	1.35		N/A		
E002	Pos.	47.70	42.95	0.73	2.08	13.89	2.37	2.90	1.94
	Neg.	46.80	42.27	0.53	2.84		2.32	2.84	1.88
E002-R	Pos.	37.35	34.87	0.90	1.36	13.29	N/A		
	Neg.	35.25	32.48	0.74	1.54		N/A		

*DOL: Direction of loading

diagonal cracks. In such cases, the principal tensile stress is lower than the tensile strength of the joint. Thus, the diagonal crack occurs when the principal tensile stress exceeds the tensile strength of concrete. As a conclusion, failure of joint is limited by the tensile strength of concrete, which can be formulated by $0.5\sqrt{f_c^*}$ (İlki *et al.* 2011). Principal stresses can be calculated by using Mohr Theorem. The maximum and minimum normal stresses are the highest and lowest points of circle which has a radius, R, on the horizontal axis. The magnitude of principal stresses is given by Mohr Theorem are represented in Eq. (4).

$$\sigma_{1,2} = \frac{\sigma_x - \sigma_y}{2} \pm \sqrt{\left(\frac{\sigma_x - \sigma_y}{2}\right)^2 + \tau_{xy}^2} \quad (4)$$

The estimated horizontal joint shear stress can be calculated by Eq. (5) and estimated joint shear force is computed by multiplying Eq. (5) and cross sectional area of joint as shown in Eq. (6).

$$\tau_{xy} = 0.5\sqrt{f_c^*} \sqrt{1 + \left[\frac{\sigma_y}{0.5\sqrt{f_c^*}}\right]^2} \quad (5)$$

$$V_{jh} = \tau_{xy} A_c \quad (6)$$

The estimated effect of transverse reinforcement to the joint shear force can be obtained from Eq. (7) for the first specimen with transverse reinforcement in the joint (TS500).

$$V_t = A_{st} f_y \frac{d}{s} \quad (7)$$

The total theoretical shear capacity of the first reference specimen (E001) is the sum of Eq. (6) and Eq. (7). In E002, there was no transversal reinforcement so the shear capacity was equal to the value obtained by Eq. (6) only.

Experimentally obtained joint shear stress calculated by using Eq. (2) was compared with the predicted joint shear stress determined theoretically as well as the code specified values in Table 3. The joint stresses were given by considering the concrete compressive strength to be consistent

Table 3 Comparison of experimental and predicted joint shear stress

Test Series	Specimen Number	Experimental Joint Shear Stress (MPa)	Predicted Joint Shear Stress (MPa)	ACI (MPa)	TEC 2007 (MPa)
Series 1	E001	5.024	5.014	4.357 ^a	4.310
Series 2	E002	2.370	1.859	0.967 ^b	3.339

^aACI 352-2002^bACI 352-1976

with the code values.

Since E001 was designed according to earthquake code in action in Turkey, the experimental results should be compared with the current codes such as ACI 352-2002 (American Concrete Institute (ACI) 2002). In E002, shear stress acting on joint was only resisted by tensile strength of concrete. However, current codes have minimum shear reinforcement at the joint region so the experimental stress of joint should be compared with noncurrent code which is ACI 352-1976 and considers only tensile strength of concrete in the joint (American Concrete Institute (ACI) 1976).

5. Conclusions

In this study, the response of two full-scale beam-column assemblies was investigated experimentally under the combined effect of axial and horizontal loading. The first specimen was designed according to the current earthquake code principles, whereas the second specimen contains several deficiencies resulting from the lack of transverse reinforcement in the joint and poor material properties such as low strength concrete and plain round bars as reinforcement steel. Both specimens were tested under quasi static cyclic loading up to 4% drift ratio. The first specimen displayed a ductile behavior with the concentration of flexural and shear cracks mostly in the beam. The beam-column joint of the second specimen was severely damaged while the rest of the RC components were almost in their elastic range. The specimens were then structurally repaired by wrapping the damaged components by CFRP sheets with different configurations depending on the damage type. After repeating the same tests for the repaired specimens, the effectiveness of the repairing techniques applied for the damaged specimens were investigated. Based on the results obtained in this study, the following conclusions can be drawn.

- The earthquake code compliant specimen (E001) displayed a ductile response with the damage concentration in the beam while the rest of the components were mostly undamaged. The experimental results indicated that the applied repairing scheme for the damaged component of the first specimen is quite effective in terms of strength, stiffness and energy absorption capacity to attain the corresponding capacities of the reference specimen. The flexural and shear capacities of the damaged beam were recovered by wrapping the member with longitudinal CFRP sheets at the top and bottom surfaces by anchoring them with transverse CFRP sheets as to improve the shear capacity of the damaged member.

- The reference deficient beam-column assembly displayed a brittle type of failure due to the severe damage in the joint, while the rest of the components were slightly damaged. The repaired specimen improved the strength capacity of the damaged reference specimen corresponding to its final condition. However, ultimate load capacity of the reference specimen could not be attained by the applied repairing due to the fracture of diagonal CFRPs resulting from the eccentricity in

the section of CFRP sheet. Since the whole area of CFRP sheet did not work as it was designed, the tearing of the CFRP sheet caused the fracture starting from the CFRP sheet side with greater axial stress. For a further improvement in the behavior, the amount of CFRP sheets wrapped in joint should be increased.

- Although the fractured CFRPs in E002 did not improve the capacity of the reference specimen, the application of diagonal CFRPs at the beam-column joint has changed the behavior of the beam-column assembly and flexural deformations in the beam amplified and dominated the overall response before the fracture of CFRPs. This indicates that, if the fracture of CFRP sheets was prevented, more ductile behavior can be achieved.

- The initial stiffness of reference specimens is higher than the ones for repaired specimens due to pre-formed cracks occurred after testing the reference specimens. The degraded stiffness sustained at each loading cycle was also higher in the reference specimens. The dissipated energy in the first repaired specimen was almost the same with the first reference specimen for the investigated drift ratios which show the efficiency of repairing. However, in the second specimen, due to the fracture of diagonal CFRP sheets at the joint, the energy dissipated in the repaired specimen is less than the reference specimen. Therefore, more layers of diagonal CFRP sheets should be applied in order to prevent the fracture of CFRPs due to eccentric stress distribution.

- The shear strains measured from the experiment decreased in the second repaired specimen before the fracture of CFRPs compared to the second reference specimen. Therefore, the deformation in the beam-column joint region has diminished with the employed repairing technique. However, the situation is just the opposite for the first specimen. With the application of CFRP sheets at the beam and column only, the deformations in the joint increased compared to the first reference specimen. This indirectly indicates the effectiveness of the repairing technique for E001 by improving the damaged beam and hence observed deformations in the beam was less. Improvement in the beam deformations lead to increase in the deformations of unrepaired components, which is the beam-column joint in this case.

- The test results of the reference test series revealed the importance of transverse reinforcement in the beam-column joint once again. Due to the lack of joint transverse reinforcement, deficient beam-column joint can be exposed to brittle type of shear failure, which adversely affect the overall seismic behavior of the RC structures.

Acknowledgments

The support of BASF Chemical Company is gratefully acknowledged.

Funding

The research described in this paper was financially supported by Anadolu University Scientific Research Projects Commission [grant number 1210F169].

References

ACI 352R-02 (2002), *Recommendations for design of beam-column connections in monolithic reinforced*

- concrete structures, American Concrete Institute, Detroit, USA.
- ACI 352R-76 (1976), *Recommendations for design of beam-column connections in monolithic reinforced concrete structures*, American Concrete Institute, Detroit, USA.
- Akguzel, U. and Pampanin, S. (2010), "Effects of variation of axial load and bidirectional loading on seismic performance of GFRP retrofitted reinforced concrete exterior beam-column joints", *J. Compos. Constr.*, **14**, 94-104.
- Alcocer, S.M. and Jirsa, J.O. (1991), "Reinforced concrete frame connections rehabilitated by jacketing", PMFSEL Rep. No. 91-1, Phil M. Ferguson Structural Engineering Laboratory, Univ. of Texas at Austin, Austin, TX.
- Antonopoulos, C.P. and Triantafillou, T.C. (2003), "Experimental investigation of FRP-strengthened RC beam-column joints", *J. Compos. Constr.*, **7**, 39-49.
- Avşar, Ö. and Tunaboyu, O. (2014), "Influence of structural wall on the seismic performance of RC buildings during the May 19, 2011 Simav, Turkey Earthquake", *J. Perform. Constr. Facil.*, **28**(4), 04014016.
- Bedirhanoglu, I., İlki, A., Pujol, S. and Kumbasar, N. (2010), "Seismic behavior of joints built with plain bars and low-strength concrete", *ACI Struct. J.*, **107**(3), 300-310.
- Biddah, A., Ghobarah, A. and Aziz, T.S. (1997), "Upgrading of nonductile reinforced concrete frame connections", *J. Struct. Eng.*, **123**, 1001-1010.
- Bindhu, K.R., Jaya, K.P. and Manicka Selvam, V.K. (2008), "Seismic resistance of exterior beam-column joints with non-conventional confinement reinforcement detailing", *Struct. Eng. Mech.*, **30**(6), 733-761.
- Burak, B. and Wight, J.K. (2004), "Experimental investigation of eccentric reinforced concrete beam-column-slab connections under earthquake loading", *13th World Conference on Earthquake Engineering*, Vancouver, B.C., Canada.
- Canbolat, B.B. and Wight, J.K. (2008), "Experimental investigation on seismic behavior of eccentric reinforced concrete beam-column-slab connections", *ACI Struct. J.*, **16**(105-S), 154-162.
- Coskun, C., Comert, M., Demir, C. and İlki, A. (2012), "FRP retrofit of a full-scale 3D RC frame", *6th International Conference on FRP Composites in Civil Engineering (CICE 2012)*, Rome, Italy.
- Del Vecchio, C., Di Ludovico, M., Balsamo, A., Manfredi, G. and Dolce, M. (2014), "Experimental investigation of exterior RC beam-column joints retrofitted with FRP systems", *J. Comps. Constr.*, **18**(4) 04014002.
- Doğangün, A. (2004), "Performance of reinforced concrete buildings during the May 1, 2003 Bingöl earthquake in Turkey", *Eng. Struct.*, **26**(6), 841-856.
- El-Amoury, T. and Ghobarah, A. (2002), "Seismic rehabilitation of beam-column joint using GFRP sheets", *Eng. Struct.*, **24**, 1397-1407.
- Elsouri, A.M. and Harajli, M.H. (2015), "Repair and FRP strengthening of earthquake-damaged RC shallow beam-column joints", *Adv. Struct. Eng.*, **18**, 237-250.
- Engindeniz, M. (2008), "Repair and strengthening of pre-1970 reinforced concrete corner beam-column joints using CFRP composites", Ph.D. Dissertations, Georgia Institute of Technology, Georgia, USA.
- Fisher, M.J. and Sezen, H. (2011), "Behavior of exterior reinforced concrete beam-column joints including a new reinforcement", *Struct. Eng. Mech.*, **40**(6), 867-883.
- Garcia, R., Jemaa, Y., Helal, Y., Maurizio, G. and Pilakoutas, K. (2014), "Seismic strengthening of severely damaged beam-column RC joints using CFRP", *J. Comps. Constr.*, **18**(2) 04013048.
- Ghobarah, A. and El-Amoury, T. (2005), "Seismic rehabilitation of deficient exterior concrete frame joints", *J. Comps. Constr.*, **9**, 408-416.
- Ghobarah, A. and Said, A. (2001), "Seismic rehabilitation of beam-column joints using FRP laminates", *J. Earthq. Eng.*, **5**(1), 113-129.
- Ghobarah, A. and Said, A. (2002), "Shear strengthening of beam-column joints", *Eng. Struct.*, **24**, 881-888.
- Haach, V.G., Debs, A.L.H.D.C.E. and Debs, M.K.E. (2008), "Evaluation of the influence of the column axial load on the behavior of monotonically loaded RC exterior beam-column joints through numerical simulations", *Eng. Struct.*, **30**, 965-975.
- Hadi, N.S.M. and Tran, T.M. (2014), "Retrofitting nonseismically detailed exterior beam-column joints

- using concrete covers together with CFRP jacket”, *Construct. Build. Mater.*, **63**, 161-173.
- Hassan, W.M. (2011), “Analytical and experimental assessment of seismic vulnerability of beam-column joints without transverse reinforcement in concrete buildings”, Ph.D. Dissertations, University of California, Berkeley, USA.
- İlki, A., Bedirhanoglu, I. and Kumbasar, N. (2011), “Behavior of FRP-retrofitted joints built with plain bars and low-strength concrete”, *J. Compos. Constr.*, **15**, 312-326.
- Karayannis, C.G., Chalioris, C.E. and Sideris, K.K. (1998), “Effectiveness of RC beam-column connection repair using epoxy resin injections”, *J. Earthq. Eng.*, **2**(2), 217-240.
- Karayannis, C.G., Chalioris, C.E. and Sirkelis, G.M. (2008), “Local retrofit of exterior RC beam-column joints using thin RC jackets-An experimental study”, *Earthq. Eng. Struct. Dyn.*, **37**(5), 727-746.
- Karayannis, C.G. and Sirkelis, G.M. (2008), “Strengthening and rehabilitation of RC beam-column joints using carbon-FRP jacketing and epoxy resin injection”, *Earthq. Eng. Struct. Dyn.*, **37**(5), 769-790.
- Kotsovou, G. and Mouzakis, H. (2012), “Exterior RC beam-column joints: new design approach”, *Eng. Struct.*, **41**, 307-319.
- Le-Trung, K., Lee, K., Lee, J., Lee, D.H. and Wooc, S. (2010), “Experimental study of RC beam-column joints strengthened using CFRP composites”, *Compos. Part: B*, **41**, 76-85.
- Lee, J.Y., Kim, J.Y. and Oh, G.J. (2009), “Strength deterioration of reinforced concrete beam column joints subjected to cyclic loading”, *Eng. Struct.*, **41**(9), 2070-2085.
- Lee, W.T., Chiou, Y.J. and Shih, M.H. (2010), “Reinforced concrete beam-column joint strengthened with carbon fiber reinforced polymer”, *Compos. Struct.*, **92**, 48-60.
- Li, B. and Kai, Q. (2011), “Seismic behavior of reinforced concrete interior beam-wide column joints repaired using FRP”, *J. Compos. Constr.*, **15**(3), 327-338.
- Mahini, S.S. and Ronagh, H.R. (2010), “Strength and ductility of FRP web-bonded RC beams for the assessment of retrofitted beam-column joints”, *Compos. Struct.*, **92**, 1325-1332.
- Park, R. (1989), “Evaluation of ductility of structures and structural assemblages from laboratory testing”, *NZ Nat. Soc. Earthq. Eng. Bull.*, **22**(3), 155-166.
- Parvin, A. and Granata, P. (2000), “Investigation on the effects of fiber composites at concrete joints”, *Compos. Part: B*, **31**, 499-509.
- Parvin, A., Altay, S., Altay, C. and Kaya, O. (2010), “CFRP rehabilitation of concrete frame joints with inadequate shear and anchorage details”, *J. Compos. Constr.*, **14**(1), 72-82.
- Sezen, H., Whittaker, A.S., Elwood, K.J. and Mosalam, K.M. (2003), “Performance of reinforced concrete buildings during the August 17, 1999 Kocaeli, Turkey earthquake, and seismic design and construction practice in Turkey”, *Eng. Struct.*, **25**(1), 103-114.
- TEC-2007 (2007), *Specification for structures to be built in disaster areas*, Turkish Earthquake Code, Ministry of Public Works and Settlement Government of Republic of Turkey, Turkey.
- Topcu, I. (2008), “Experimental research on seismic retrofitting of R/C corner beam-column-slab joints upgraded with CFRP sheets”, MSc Thesis, Graduate Program in Civil Engineering, Bogaziçi University.
- TSI-500 (2000), *Requirements for design and construction of reinforced concrete structures*, Turkish Standards Institute, Ankara, Turkey.
- Yılmaz, N. and Avcı, Ö. (2013), “Structural damages of the May 19, 2011 Kütahya-Simav Earthquake in Turkey”, *Nat. Hazard.*, **69**(1), 981-1001.

CC

Notations

f_c^* = Standard cylindrical concrete compressive at experiment date
 f_y = Yield strength of steel

f_u =Ultimate strength of steel
 A_c =Gross cross-sectional area of column, beam and joint
 V_{max} =Maximum lateral load that observed during experiment
 Δ_u =Ultimate displacement that corresponds 20% reduction of maximum lateral load
 V_y =Yield load of specimens
 Δ_y =Yield displacement of specimens
 Δ_y^* =Yield drift ratio of specimens
 K =Initial stiffness
 K^p =Peak to peak stiffness
 E =Dissipated energy
 σ_t =Experimental value of principal tensile strength in joint
 σ_c =Experimental value of principal compression strength in joint
 $\sigma_{1,2}$ =Predicted principal tensile strength in joint, $0.5\sqrt{f_c^*}$
 σ_x =Normal stress in the beam
 σ_y =Normal stress in the column
 τ_{xy} =Predicted shear stress in the joint
 V_{jh} =Estimated joint shear force
 τ_j =Experimental joint shear stress
 V_b =Beam horizontal force in the beam longitudinal reinforcement bars
 V_c =Column tip load at any displacement
 V_j =Experimental joint shear force
 γ =Joint shear strain
 L_v =Sum of gauge length and measured displacement of vertical LVDTs
 L_h =Sum of gauge length and measured displacement of horizontal LVDTs
 L_d =Sum of gauge length and measured displacement of diagonal LVDTs
 N =Axial load
 V_t =Contribution of transverse reinforcement to the joint shear force
 A_{st} =Area of stirrup in the joint
 s =Spacing of transversal reinforcement in the joint
 d =distance from extreme compression fiber to centroid of longitudinal tension reinforcement